Self-Organization Phenomena

Deutsche Ausgabe: DOI: 10.1002/ange.201607030
Internationale Ausgabe: DOI: 10.1002/anie.201607030

# Self-Organized Stationary Patterns in Networks of Bistable Chemical Reactions

*Nikos E. Kouvaris,* Michael Sebek, Alexander S. Mikhailov, and István Z. Kiss*

***Abstract:*** *Experiments with networks of discrete reactive bistable electrochemical elements organized in regular and nonregular tree networks are presented to confirm an alternative to the Turing mechanism for the formation of self-organized stationary patterns. The results show that the pattern formation can be described by the identification of domains that can be activated individually or in combinations. The method also enabled the localization of chemical reactions to network substructures and the identification of critical sites whose activation results in complete activation of the system. Although the experiments were performed with a specific nickel electrodissolution system, they reproduced all the salient dynamic behavior of a general network model with a single nonlinearity parameter. Thus, the considered pattern-formation mechanism is very robust, and similar behavior can be expected in other natural or engineered networked systems that exhibit, at least locally, a treelike structure.*

In a biological context, many chemical reactions take place in discrete units, such as cells, that form a complex network.[1] Similarly, advances in microfabrication enable the generation of engineered networks of reaction units, for example, with lab-on-chip microdroplets,[2] electrode arrays,[3,4] or BZ beads.[5] The interplay between local reaction kinetics (nodes), the physical processes that create coupling (links), and the architecture of the network in such systems can lead to a wealth of self-organization phenomena, including synchronization,[5] stationary Turing patterns,[6–8] and excitation waves.[9,10]

Stationary patterns generated by the Turing[11] mechanism have been observed in experiments for both continuous systems[12] and complex networks.[13] Herein, an alternative mechanism for the emergence of stationary patterns in networks is explored experimentally. We focus on network-organized systems of bistable elements with diffusive connections between them. Bistable elements can be found in a broad class of chemical reactions (e.g., with autocatalysis[14]), but also in cellular[15] and engineered systems.[16] Such elements can have local connections between them. For regular lattices and linear chains (i.e., for relatively simple networks), it is known that, under sufficiently weak coupling, the fronts fail to propagate, and thus stationary domains can be formed,[17–21] whereas with strong coupling the fronts spread[20,21] and a uniform state is eventually established. Recently, analogous phenomena were theoretically investigated for complex networks, and the formation of stationary domains, sensitive to the network topology, was predicted on the basis of a simple model of regular trees and one-component bistable elements.[22,23] The aim of the present study is to experimentally identify the stationary-pattern formation induced by a discrete network structure, with chemical reactions in which autocatalysis can produce local bistable behavior.

Suppose that some substance can undergo chemical reactions in reactors occupying nodes $i$ ($i = 1, \ldots, N$) of a network, and that this substance can spread diffusively from one node to another. Such a network-organized reaction-diffusion system is generally described by equations $\dot{u}_i = f(u_i) + K\sum_j A_{ij}(u_j - u_i)$, in which $u_i$ is the chemical concentration in the node $i$, the function $f(u)$ specifies the local dynamics at the nodes, and the coefficient $K$ characterizes the strength of diffusive coupling. The network structure is determined by a symmetric adjacency matrix whose elements are $A_{ij} = 1$ if there is a connection between nodes $i$ and $j$ ($i \neq j$), and $A_{ij} = 0$ otherwise. Function $f(u)$ can be chosen in such a way that individual elements are bistable, for example, owing to autocatalysis (see the Supporting Information). For such models, an approximate analytical theory is available for regular trees with a fixed branching ratio.

Under given nonlinearity conditions (see the Supporting Information), the two major parameters are the coupling strength $K$ and the branching ratio $r$. For weak coupling, the activation is pinned (i.e., it does not propagate) in region I (see Figure 1 a). At an intermediate coupling strength, there is a range of branching ratios (region II), where the center activation is pinned, while the periphery activation propagates towards the center. For sufficiently strong coupling and relatively low branching ratios (region III), the center activation spreads towards the periphery, whereas the periphery activation propagates towards the center. At strong coupling and large branching ratios (region IV), the center activation retreats, and the periphery activation propagates towards the center. The behavior of regular or nonregular tree networks can be interpreted fully in terms of these four regions.

Figure 1 b shows a nonregular tree network with branching ratios varying from one to two, three, four, and five.

[*] Dr. N. E. Kouvaris
Department of Physics, University of Barcelona
Martí i Franquès 1, 08028 Barcelona (Spain)
E-mail: nikos.kouvaris@upf.edu

M. Sebek, Prof. I. Z. Kiss
Department of Chemistry, Saint Louis University
3501 Laclede Avenue, St. Louis, Missouri 63103 (USA)

Prof. A. S. Mikhailov
Department of Physical Chemistry
Fritz Haber Institute of the Max Planck Society
Faradayweg 4–6, 14195 Berlin (Germany)

Supporting information and the ORCID identification number(s) for the author(s) of this article can be found under http://dx.doi.org/10.1002/anie.201607030.

  

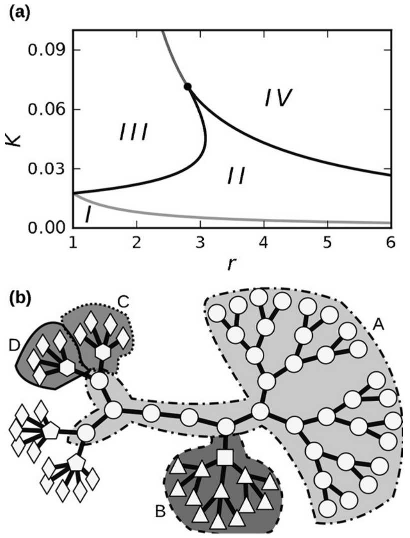


*Figure 1.* a) Bifurcation diagram. Region I: Activations are pinned. Region II: Center activation is pinned, whereas periphery activation propagates towards the center of the tree. Region III: Center and periphery activations propagate. Region IV: Center activation retreats, whereas periphery activation propagates. b) Active domains *A*, *B*, *C*, and *D* are distinguished by different shades of gray. The activation of any node shown by a circle, triangle, or hexagon results in spreading of the activation over all nodes in the respective network domains *A*, $A \cup B$, $A \cup C$, or $A \cup D$. The activation of any node shown by a square or rhombus remains pinned. The activation of a single node shown by a pentagon retreats and vanishes, thus resulting in the uniform passive state.

Numerical simulations for this network were performed with the coupling constant $K = 0.04$, so that these domains corresponded to regions II, III, and IV in the bifurcation diagram. Simulations were carried out by applying initial activation to one of the nodes and following the subsequent evolution until a stationary state was reached. Stationary patterns were then classified by identifying all the possible stationary states that could be obtained by such an initial activation.

The developed patterns can be interpreted by the formation of domains activated individually or in combinations. The domains consist of groups of nodes that correspond to the same dynamic region and thus behave similarly. For example, domains of elements in region III support the spreading of activation towards both the center and the periphery. When such domains are adjacent to or surrounded by nodes that are amenable to pinning or to retreating (e.g., in region I, II, or IV) the propagating fronts get pinned, and stationary structures develop. Therefore, the observed structures consist of uniform domains separated by nodes amenable to pinning or to retreating. The exact configuration of the patterns depends on the architecture of the network, the applied coupling strength, and the nonlinearity of the reaction, which together determine the assignment of the nodes to the different regions and the configuration of the domains.

For the specific network shown in Figure 1b, the activation of any node shown by a circle, triangle, or hexagon resulted in the spreading of activation to all nodes of the domains $A$, $A \cup B$, $A \cup C$, or $A \cup D$. The activation of any node shown by a square or rhombus remained pinned on that node. The activation of a node shown with a pentagon retreated and vanished, thus resulting in the uniform final passive state. Simulations were also performed by initially activating several network nodes, but essentially the same final patterns were then reached.

Experiments with networks of reactive bistable electrochemical elements were performed (see the Supporting Information). Each unit represented a corroding metal (nickel) wire that accommodated a complex reaction system (including the formation of multiple forms of metal oxides, bisulfate adsorption, oxygen evolution, and metal dissolution) that exhibited bistable behavior. The active state corresponds to a high current, and the passive state to a low current. Moreover, coupling was established in the form of a charge flow between the wires (owing to the difference in electrode potential), which affected the rate of metal dissolution of the coupled electrodes. Electrodes and external connections between them correspond to the nodes and the links in all network diagrams.

First, experiments with regular trees were undertaken. As shown in Figure 2, center activation in a four-layer tree with the branching ratio 3 could result in spreading fronts (Figure 2b, region III) for weak coupling, pinned fronts (Figure 2c, region II) for moderate coupling, and retreating fronts (Figure 2d, region IV) for strong coupling. Similarly, periphery activation (Figure 2e) yielded either pinned fronts (Figure 2e, region I) at very weak coupling or spreading fronts (Figure 2 f) at stronger coupling; such behavior was found in all regions II, III, and IV.

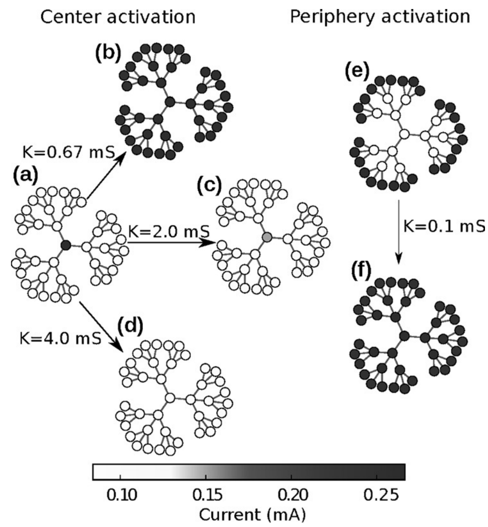


*Figure 2.* Evolution of center and periphery activations on a regular tree with a branching ratio $r=3$ at different coupling strengths $K$. a) Initial condition of center activation. b) Spreading front, $K=0.67$ mS; the final state at $t=1008$ s is shown. c) Pinned front, $K=2.0$ mS, $t=2310$ s. d) Retreating front, $K=4.0$ mS, $t=68$ s. e) Initial condition of periphery activation. If $K=0.04$ mS, the front is pinned, $t=480$ s. f) Spreading front, $K=0.10$ mS, $t=464$ s, $V=1300$ mV.

  

Figure 3 shows the evolution observed in the same network after the activation of intermediate nodes at different coupling strengths. In region I (Figure 3a), the fronts are pinned on both sides. In region II (Figure 3b), the center-facing front spreads towards the center, and the periphery-facing front is pinned. In region III, fronts spread in both directions and finally activate the entire network (Figure 3c).

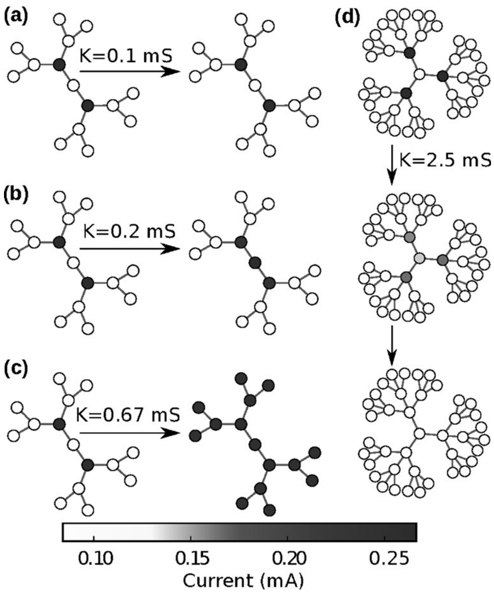


***Figure 3.*** a) Pinned fronts in both directions, $K=0.10$ mS; the final state at $t=402$ s is shown. b) The center-facing front spreads towards the center, and the periphery-facing front is pinned; $K=0.20$ mS, $t=602$ s. c) Spreading fronts in both directions, $K=0.67$ mS, $t=538$ s. d) The center-facing front spreads towards the center, and the periphery-facing front retreats from the periphery; $K=2.57$ mS, middle snapshot at $t=25$ s and final state at $t=50$ s, $V=1300$ mV.

In region IV, the center-facing front propagates towards the center, but the periphery-facing front retreats from the periphery finally establishing a passive state in the entire network (Figure 3d). All these experiments confirm the theoretical predictions for regular tree networks.

Furthermore, we could also build the same nonregular tree as in the simulations in Figure 1b. By performing experiments with regular trees under the same experimental setup, we found that at $K\approx 1$ mS, regions II, III, and IV correspond to the branching ratios $r=3$, 4, $r=1$, 2, and $r\geq 5$, respectively (see Figure S2 in the Supporting Information). Similarly to theoretical predictions, we could see that activation with a single (Figure 4a; see also Video S1 in the Supporting Information) or multiple nodes (Figure 4b; see also Video S2) within domain $A$ resulted in the activation of all elements in domain $A$. When activation was applied to an intermediate element of domain $B$, pattern $A\cup B$ was observed (Figure 4c; see also Video S3). For complete activation of the network, peripheral nodes of the branches with the highest branching ratios $r=3$, 4, and 5 had to be initially activated (Figure 4d; see also Video S4). When a root node of a branch with a high branching ratio of $r=4$ or 5 was

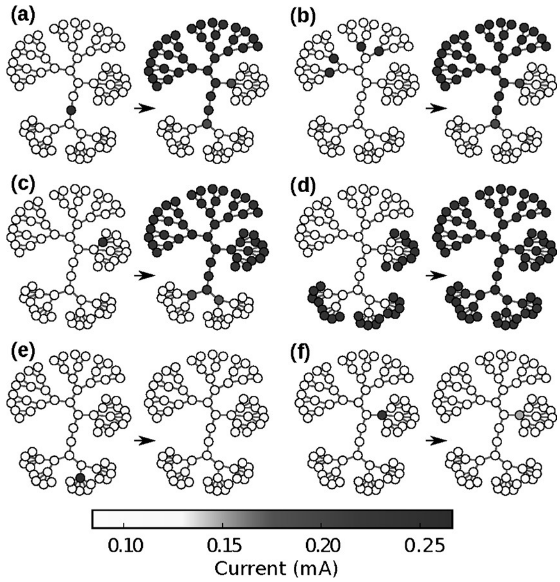


***Figure 4.*** a) The activation of a single node in domain $A$ yields spreading fronts that activate this domain ($V=1300$ mV, final state at $t=654$ s). b) The intermediate activation of four nodes in domain $A$ with $r=2$ yields spreading fronts that activate domain $A$ ($V=1295$ mV, final state at $t=241$ s). c) Near-periphery activation of a single node in the branch with $r=3$ yields spreading fronts that activate the domains $A\cup B$ ($V=1275$ mV, final state at $t=336$ s). d) Periphery activation of the branches with $r=3$, 4, and 5 yields spreading fronts to complete network activation ($V=1280$ mV, final state at $t=201$ s). e) The activation of a single node in the branch with $r=5$ yields retreating fronts to complete network passivation ($V=1300$ mV, final state at $t=54$ s). f) The activation of a single more central node in the branch with $r=3$ yields pinned fronts ($V=1270$ mV, final state at $t=801$ s). All experiments were performed at $K=1.3$ mS.

initially activated, the activation could not spread and died out (Figure 4e). Furthermore, the activation of a more central node in the branch with $r=3$ resulted in a pinned front (Figure 4f).

Many features of the stationary patterns in a large, nonregular network can be predicted from the network topology on the basis of experiments with four-layer trees that identify the dependence of the dynamic behavior as a function of the branching ratio. We performed the experiments with an electrochemical system; nonetheless, a surprisingly good agreement with theoretical predictions was found despite the fact that the experimental system did not perfectly meet the idealizations made in the theory, that is, the state of a network element was described by more than a single variable, and coupling between the elements was local, but not through diffusion. Our results thus indicate that the found behavior is generic and robust; therefore, it can be expected in various natural and engineered bistable networks, such as supercomputer networks and nephrons of the kidney.[24]

Although only tree networks were considered, our results are also relevant for large random networks that possess the tree structure locally with relatively short-range effective interactions among the elements. Hence, the formation of stationary domains should also be a characteristic property of random networks, provided that such domains remain sufficiently small. Finally, as has been shown theoretically,[23] self-organized stationary domains can be controlled by introducing possibilities for global feedback, and such control would further facilitate the design of complex stationary structures on networks.

## Acknowledgements

N.E.K. acknowledges financial support by the LASAGNE (Contract No. 318132) EU project. M.S. and I.Z.K. acknowledge support from the National Science Foundation (CHE-1465013).

**Keywords:** autocatalysis · bistability · complex networks · electrochemistry · pattern formation

**How to cite:** *Angew. Chem. Int. Ed.* **2016**, *55*, 13267–13270
*Angew. Chem.* **2016**, *128*, 13461–13464

[1] L. R. Varshney, B. L. Chen, E. Paniagua, D. H. Hall, D. B. Chklovskii, *PLoS Comp. Biol.* **2011**, *7*, e1001066.
[2] M. Toiya, V. G. Vanag, I. R. Epstein, *Angew. Chem. Int. Ed.* **2008**, *47*, 7753; *Angew. Chem.* **2008**, *120*, 7867.
[3] M. Wickramasinghe, I. Z. Kiss, *PloS ONE* **2013**, *8*, e80586.
[4] Y. Jia, I. Z. Kiss, *J. Phys. Chem. C* **2012**, *116*, 19290.
[5] M. R. Tinsley, S. Nkomo, K. Showalter, *Nat. Phys.* **2012**, *8*, 662.
[6] W. Horsthemke, K. Lam, P. K. Moore, *Phys. Lett. A* **2004**, *328*, 444.
[7] H. Nakao, A. S. Mikhailov, *Nat. Phys.* **2010**, *6*, 544.
[8] N. E. Kouvaris, S. Hata, A. Díaz-Guilera, *Sci. Rep.* **2015**, *5*, 10840.
[9] N. E. Kouvaris, T. Isele, A. S. Mikhailov, E. Schöll, *Europhys. Lett.* **2014**, *106*, 68001.
[10] A. J. Steele, M. Tinsley, K. Showalter, *Chaos* **2006**, *16*, 015110.
[11] A. M. Turing, *Philos. Trans. R. Soc. London* **1952**, *237*, 37.
[12] J. Horvath, I. Szalai, P. De Kepper, *Science* **2009**, *324*, 772.
[13] N. Tompkins, N. Li, C. Girabawe, M. Heymann, G. B. Ermentrout, I. R. Epstein, S. Fraden, *Proc. Natl. Acad. Sci. USA* **2014**, *111*, 4397.
[14] I. R. Epstein, J. A. Pojman, *An Introduction to Nonlinear Chemical Dynamics: Oscillations, Waves, Patterns, and Chaos*, Oxford University Press, Oxford, **1998**.
[15] T. G. W. Graham, S. M. Ali Tabei, A. R. Dinner, I. Rebay, *Development* **2010**, *137*, 2265.
[16] K. Ikeda, H. Daido, O. Akimoto, *Phys. Rev. Lett.* **1980**, *45*, 709.
[17] V. Booth, T. Erneux, *Physica D* **1992**, *188*, 206.
[18] T. Erneux, G. Nicolis, *Physica D* **1993**, *67*, 237.
[19] I. Mitkov, K. Kladko, J. Pearson, *Phys. Rev. Lett.* **1998**, *81*, 5453.
[20] J. P. Laplante, T. Erneux, *Physica A* **1992**, *188*, 89.
[21] G. Flätgen, K. Krischer, *Phys. Rev. E* **1995**, *51*, 3997.
[22] N. E. Kouvaris, H. Kori, A. S. Mikhailov, *PLoS ONE* **2012**, *7*, e45029.
[23] N. E. Kouvaris, A. S. Mikhailov, *Europhys. Lett.* **2013**, *102*, 16003.
[24] a) J. R. Goodman, C. H. Sequin, *IEEE Trans. Comp.* **1981**, *C-30*, 923; b) D. D. Postnov, D. E. Postnov, D. J. Marsh, N. H. Holstein-Rathlou, O. V. Sosnovtseva, *Bull. Math. Biol.* **2012**, *74*, 2820.

Received: July 20, 2016
Published online: September 21, 2016

  